Available online at www.sciencedirect.com

SCIENCE DIRECT®

Journal of Catalysis 238 (2006) 122–133

JOURNAL OF CATALYSIS

www.elsevier.com/locate/jcat

Initial stages of propane activation over Zn/MFI catalyst studied by in situ NMR and IR spectroscopic techniques

Yu.G. Kolyagin [a], V.V. Ordomsky [a], Y.Z. Khimyak [b], A.I. Rebrov [c], F. Fajula [d], I.I. Ivanova [a,*]

[a] *Department of Chemistry, Moscow State University, Lenin Hills 1, Bld. 3, 119992 Moscow, Russia*
[b] *Department of Chemistry, University of Liverpool, Liverpool L69 7ZD, UK*
[c] *Institute of Petrochemical Synthesis, RAS, Leninsky pr. 29, 117012 Moscow, Russia*
[d] *UMR 5618 ENSCM/CNRS/UM1, 8 Rue de l'Ecole Normale, 34296 Montpellier cedex, France*

Received 12 September 2005; revised 21 November 2005; accepted 26 November 2005

Available online 9 January 2006

Abstract

The early stages of propane activation over Zn-modified H-MFI catalysts were studied by in situ ^{13}C MAS NMR and IR spectroscopic techniques. Propane 2-^{13}C, propane 1-^{13}C, deuterated propane, and deuterated dihydrogen were used as labelled reactants. Both techniques pointed to the formation of zinc propyl species at the onset of propane conversion. Moreover, formation of ZnOH groups simultaneously to zinc propyl species was evidenced by IR spectroscopic techniques. The results point to the propane activation through dissociative adsorption over zinc oxide species, followed by propene evolution and recombinative desorption of dihydrogen. Propene further oligomerizes over acidic sites, while dihydrogen either evolves as a final product or participates in propane hydrogenolysis into ethane and methane. At low partial pressure of reactants, H_2 recombinative desorption and hydrogen evolution are favoured, whereas at high pressures, the hydrogenolysis route is preferable.
© 2005 Elsevier Inc. All rights reserved.

Keywords: Zn-containing MFI zeolites; Propane conversion; Mechanism of propane activation; In situ FTIR and ^{13}C MAS NMR spectroscopies

1. Introduction

The conversion of light alkanes to aromatics requires bifunctional catalysts involving both acidic and dehydrogenation functions. The best catalysts proposed so far are based on acidic MFI zeolites modified with Ga or Zn. Understanding the interplay between the acidic and dehydrogenation catalytic functions in these catalysts is of key importance to further improving their selectivity, activity, and lifetime. But despite numerous extensive studies, the catalytic role of acidic sites as well as Ga and Zn species, especially at the early stages of alkanes activation, remains controversial.

According to Ono et al. [1], the initial step in propane activation involves acidic sites only implying carbonium ion mechanism, while the "metal" sites are participating in olefin-to-aromatics conversion with no influence on the initial stages of propane transformation. In contrast, Guisnet et al. [2] proposed that "metal"-containing sites play the main role in the initial propane dehydrogenation leading to propene, which is further converted to higher hydrocarbons over acidic sites. Price et al. [3] proposed that on MFI catalyst fully exchanged with gallium, acid–base pairs of Ga^+ and neighbouring basic oxygen anions associated with the zeolite framework could be responsible for propane dehydrogenation and further propene oligomerization and aromatization. Mole et al. [4] pointed out that zinc oxide can produce heterolytic cleavage of the carbon–hydrogen bond, leading to (Zn–H) species. Kazansky et al. proposed that the initial step on Zn-containing catalysts proceeds through propane dissociative adsorption, resulting in formation of zinc alkyl and acidic hydroxyl fragments [5].

In addition, numerous studies have determined a synergetic action of metal-containing and acidic sites at the initial stages of propane activation. Naccache et al. [6] and Buckles et al. [7] suggested that the first step in propane activation involves dissociative adsorption with the formation of gallium hydride (Ga–H) and gallium alkoxide (Ga–O–C_3H_7), after which rapid

---

[*] Corresponding author.
E-mail address: iivanova@phys.chem.msu.ru (I.I. Ivanova).

0021-9517/$ – see front matter © 2005 Elsevier Inc. All rights reserved.
doi:10.1016/j.jcat.2005.11.037

exchange of the propyl carbenium ions with zeolite protons through an alkyl surface migration occurs. The final step is propylene desorption and liberation of acidic sites.

Another type of synergetic mechanism was proposed by Inui et al. [8], le van Mao et al. [9], and Iglesia et al. [10], who performed kinetic and isotopic tracer studies on Zn- and Ga-modified H-MFI catalysts. These studies suggested that metal cations catalyze the recombinative desorption of H atoms as H_2 through formation of the intermediate "metal"-H species, while the initial CH cleavage occurs on the acid sites. The recombinative desorption of hydrogen species shifts the equilibrium towards the formation of propylene and suppresses hydrogen transfer to hydrocarbon species, leading to ethane and methane.

The development of in situ MAS NMR spectroscopic techniques [11] has allowed monitoring of the catalytic transformations directly on a catalyst surface during the course of the reaction. These techniques have turned out to be very informative in the mechanistic catalytic studies over heterogeneous catalysts, particularly zeolite catalysts.

Application of in situ ^{13}C MAS NMR spectroscopy has enabled identification of the proposed detailed bifunctional mechanism of propane activation over Ga-modified acidic MFI zeolite [11a,11c,11e,12]. This mechanism implies synergetic action of acidic and (Ga^{3+}–O^{-2}) ion pair sites in the formation of the protonated pseudocyclopropane (PPCP) intermediate, which further decomposes into propene and dihydrogen, methane and ethene or recombines back to propane [11a,11c,11e,12].

In contrast to Ga-containing zeolites, only few in situ ^{13}C MAS NMR data are available for zinc-modified catalyst [13]. These data point to a different reaction pathway on Zn/H-MFI catalysts, involving hydrogenolysis of propane. Further studies are needed to gain deeper insight into the mechanism of these transformations.

This paper is devoted to the investigation of the initial stages of propane transformations over Zn/H-MFI and Zn/silicalite catalysts using in situ ^{13}C MAS NMR and IR spectroscopic techniques. The results are compared with those obtained previously over H-MFI and Ga/H-MFI catalysts.

2. Experimental

Preparation of Zn-containing MFI catalysts (Zn/H-MFI, Zn/silicalite) was carried out by the impregnation with aqueous solution of $Zn(NO_3)_2$, subsequent drying at 393 K for 15 h, and calcination at 823 K for 12 h. Zeolites with $Si/Al = 35$ (H-MFI) and $Si/Al = 2000$ (silicalite) were used as starting materials. The hydrogen form (H-MFI) was obtained from the sodium form through triple ion exchange with a 0.1 M aqueous solution of NH_4NO_3 and subsequent calcination at 823 K for 6 h. The zinc content was 8.0 wt% in both samples. Ga/H-MFI catalyst was prepared from H-MFI by aqueous impregnation with $Ga(NO_3)_3 \cdot 9H_2O$, followed by drying for 16 h at 393 K and calcination at 823 K for 4 h in air. The final catalyst contained 1.5 wt% of gallium.

The materials were characterized by elemental analysis; XRD; SEM; UV–vis diffuse reflectance spectroscopy; solid-state ^{1}H, ^{27}Al, and ^{29}Si MAS NMR spectroscopy; nitrogen adsorption; and FTIR of adsorbed pyridine and CO. The elemental analysis of zeolites was performed by atomic absorption. The XRD patterns were obtained with a DRON-3M diffractometer, using Cu-K_α radiation. SEM images were obtained on CAMSCAN electron microscope. UV–vis diffuse reflectance spectra were measured on a Specord M-40 equipped with reflectance accessories. ^{1}H, ^{27}Al and ^{29}Si MAS NMR experiments were performed on a Bruker MSL 400 spectrometer. Sorption-desorption isotherms of nitrogen were measured at 77 K using an automated porosimeter (Micromeritics ASAP 2000).

^{13}C MAS NMR measurements were carried out on ADX-200 and ADVANCE DSX400 Bruker spectrometers operating at 50.3 and 100.6 MHz, respectively. Quantitative conditions were achieved using high-power gated proton decoupling with suppressed NOE effect (90° pulse, 6 s recycle delay). The experiments involving cross-polarization from protons to carbon (^{1}H–^{13}C CP MAS) were recorded with a 1-ms contact time and a 3.0-s recycle delay. Chemical shifts were referenced relatively to the CH_2 group of solid adamantane [14,15].

Controlled-atmosphere experiments were performed in sealed pyrex NMR cells containing catalysts and adsorbates and fitting precisely into 7-mm Bruker zirconia rotors. Propane 1-^{13}C (99,9% enriched) and propane 2-^{13}C (99,9% enriched), purchased from ICON Services, were used as labelled reactants. In a typical NMR experiment, the sealed NMR cell was rapidly heated to the selected temperature and maintained at this temperature for a given period. In all NMR experiments, the amount of adsorbed labelled compound was calculated on the basis of 1 molecule of adsorbate per unit cell of zeolite. The NMR spectrum was recorded after quenching of the sample cell down to 293 K. A more detailed description of in situ MAS NMR experiments has been given elsewhere [16].

IR spectra were recorded on a Nicolet Protégé FTIR spectrometer at 4 cm^{-1} optical resolution with one level of zero-filling for the Fourier transform. Before measurement, the catalysts were pressed in self-supporting discs (diameter: 1.6 cm, 7 $mg\,cm^{-2}$) and activated in the IR cell (attached to a vacuum line) at 723 K for 4 h up to 10^{-5} Torr. The adsorption of gaseous hydrogen, CO, propylene, and propane was carried out at ambient temperature. Pyridine was adsorbed at 423 K. Propane and propylene were purified before the adsorption by three pump–freeze cycles. The pressure of the adsorbed gases was measured by a Varian gauge. The spectra were recorded after adsorption, after heating to a selected temperature and subsequent evacuation at ambient temperature, to monitor the most strongly adsorbed species. The sample temperature during the treatment was monitored by a chromel–alumel thermocouple inserted into the heater of the cell.

Deuterated zeolite samples were prepared directly in the IR cell through H/D exchange with D_2O. The samples were activated as described above, cooled to 523 K, subjected to 10 Torr of D_2O, and maintained at these conditions for 30 min. Then the cell was evacuated up to 10^{-3} Torr. This procedure was repeated four times, and then the samples were activated once again before adsorption of reactants. Deuterated propane

(98%), purchased from Cambridge Isotope Laboratories, was used as a reactant in experiments over deuterated catalysts.

3. Results and discussion

3.1. Characterization of Zn/MFI catalysts

The starting materials used for the preparation of Zn-containing catalysts were characterized by XRD, SEM, ^{27}Al and ^{1}H MAS NMR, nitrogen adsorption, and FTIR spectroscopy of adsorbed pyridine. The XRD data confirmed the MFI type structure of both starting materials. SEM images revealed that H-MFI and silicalite samples had the same morphology and crystal size, ~0.5 µm. ^{27}Al MAS NMR indicated the absence of extra-framework aluminum. FTIR spectra in the OH stretching region (Fig. 1) suggested that H-MFI contained Brønsted acid groups (3610 cm^{-1}) associated with framework aluminum [Si(OH)Al], isolated external silanol groups (3745 cm^{-1}), free internal silanol groups (3730 cm^{-1}), and delocalized hydrogen-bonded groups (3500 cm^{-1}) of lattice defects:

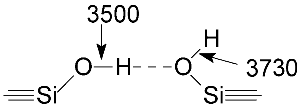

The bands assignment was as described previously [17]; ^{1}H and ^{29}Si MAS NMR data confirmed these assignments. Chemisorption of pyridine on H-MFI led to a conversion of Bronsted acid sites into pyridinium ions characterized by the band at 1546 cm^{-1}, and indicated the formation of a small amount of Lewis sites (1455 cm^{-1}) due to zeolite dehydroxylation (Fig. 2). The silicalite sample exhibited only silanol groups, which do not interact with pyridine.

Modification with zinc led to the appearance of two bands in the UV–vis diffuse reflectance spectra of H-MFI at about 265 and 375 nm. According to [18], these bands correspond to subnanomeric ZnO clusters inside zeolitic pores and large ZnO crystals on the external surface of the zeolite, respectively.

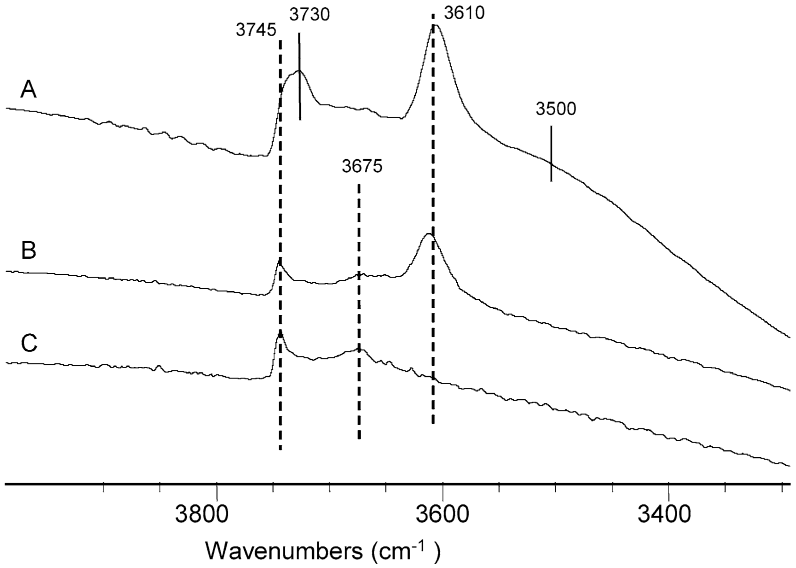

Fig. 1. FTIR spectra of hydroxyl groups of H-MFI (A), Zn/H-MFI (B), and Zn/silicalite (C) after evacuation at 723 K for 4 h.

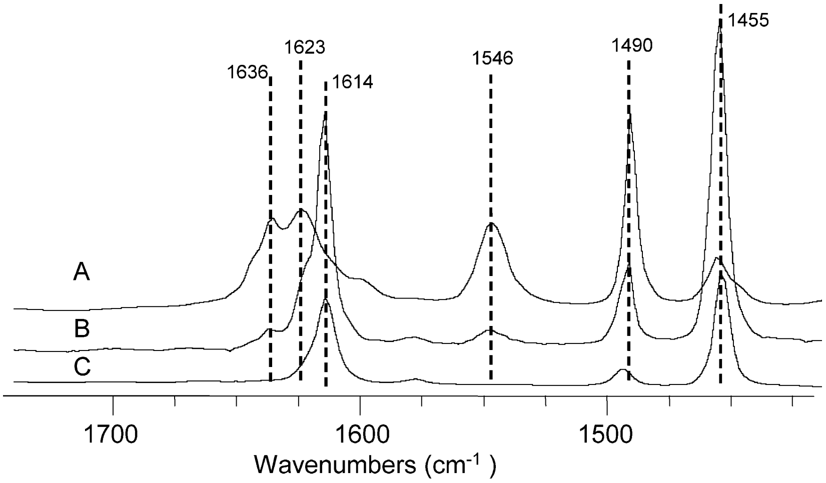

Fig. 2. FTIR spectra of pyridine adsorbed on H-MFI (A), Zn/H-MFI (B), and Zn/silicalite (C) after evacuation at 723 K for 4 h.

The content of large ZnO crystals was determined from XRD as described previously [19]. In Zn/H-MFI, it amounted to 5% of the total amount of Zn introduced (0.4 wt% in the sample), whereas in Zn/silicalite it corresponded to ∼25% of Zn (2 wt% in the sample). The nitrogen adsorption data confirmed the decrease of pore volume by ∼10% due to deposition of ZnO particles inside the pores of H-MFI and silicalite. ^{27}Al MAS NMR indicated that after dealumination of H-MFI occurred after modification with zinc.

The FTIR spectra in the OH stretching region (Fig. 1) and ^{1}H MAS NMR data (not shown) obtained on Zn/H-MFI sample pointed to a significantly decreased number of Brønsted acid groups (Si(OH)Al) on modification with Zn, suggesting consumption of zeolite protons in the exchange process. Moreover, modification led to disappearance of the internal silanol groups (3730 and 3500 cm^{-1}). El-Malki et al. [17] proposed that this is due to the interaction of internal SiOH groups with ZnOH^{+} cations located in cationic positions of the zeolite, leading to formation of (ZO)$^{-}$ Zn^{+}–O–Si species

$$(\mathrm{ZO})\text{–}\mathrm{ZnOH}^{+} + \mathrm{HO}\text{–}\mathrm{Si} \rightarrow (\mathrm{ZO})^{-}\mathrm{Zn}^{+}\text{–}\mathrm{O}\text{–}\mathrm{Si}.$$

For Zn/silicalite, the appearance of a new band at 3675 cm^{-1} was observed, most likely due to the formation of external Zn–OH groups on ZnO clusters. Small numbers of such groups were also observed on Zn/H-MFI.

The FTIR spectrum of pyridine adsorbed on Zn/H-MFI (Fig. 2) also points to the consumption of Brønsted acid sites after modification and indicates the formation of Lewis acid sites induced by the presence of zinc ions, evidenced by the appearance of the intensive band at 1455 cm^{-1}. These observations confirm that ion exchange for zinc ions occurs after modification. The comparison of relative intensites of the bands at 1546 cm^{-1}on H-MFI and Zn/H-MFI suggests that ∼80% of protons are involved in ion exchange for zinc cations. Assuming that each Al atom generates a Brønsted site in H-MFI (an hypothesis supported by the absence of extra-framework aluminum) and supposing that the protons are replaced by monopositive ZnOH^{+} cations, the maximum content of Zn in cationic positions was estimated. It appears that it may amount to 2.6 wt% in Zn/H-MFI zeolite.

Adsorption of CO on Zn-silicalite and Zn/H-MFI resulted in the appearance of bands at 2220 and 2206 cm^{-1}on the former and bands at 2230, 2220, and 2206 cm^{-1} on the latter (Fig. 3). As described previously [20,21], the band at 2206 cm^{-1} can be attributed to CO adsorption on large ZnO crystals, whereas the band at 2230 cm^{-1} could be due to CO adsorption on zinc cations. The band at 2220 cm^{-1} may arise from CO complexes with small ZnO clusters.

Analysis of the foregoing results suggests that Zn/silicalite sample contains two Zn species: small ZnO clusters inside the pores and large ZnO crystals on the external surface. In contrast, Zn/H-MFI involves three types of Zn species: small and large ZnO clusters and zinc cations. The simple estimations derived from XRD data and FTIR data suggest that most of the Zn species in both samples is contained in the form of subnanomeric ZnO clusters inside the zeolitic pores.

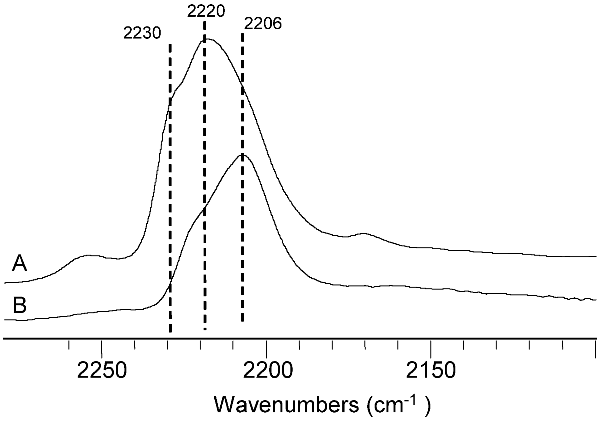

Fig. 3. FTIR spectra of CO adsorbed on Zn/H-MFI (A) and Zn/silicalite (B) after evacuation at 723 K for 4 h.

With respect to cationic species, it is difficult to determine the types of cations present in Zn/H-MFI. The literature data suggest that the most likely cationic species formed after ion exchange with nitrate solutions is ZnOH^{+}, but this species is not stable and undergoes dehydration on calcination [22]. At low Zn loading, ZnOH^{+} couples with nearby protons to form Zn^{2+} and water, which desorbs. At high Zn loadings (<1.3 wt%), ZnOH^{+} may interact with another ZnOH^{+} or a SiOH group, leading to the formation of (OZ)$^{-}$(Zn–O–Zn)$^{2+}$(OZ)$^{-}$ [22] or (ZO)$^{-}$Zn^{+}–O–Si [17], respectively. The Zn/H-MFI sample used in this study has a high Si/Al ratio and a high Zn content, and thus (OZ)$^{-}$(Zn–O–Zn)$^{2+}$(OZ)$^{-}$ or (ZO)$^{-}$Zn^{+}–O–Si cations should preferably form based on the literature data; however, the presence of Zn^{2+} or ZnOH^{+} cannot be excluded.

3.2. *Mechanistic studies*

Fig. 4a shows ^{13}C MAS NMR spectra obtained during propane 2-^{13}C reaction over the Zn/H-MFI catalyst. The initial spectrum observed immediately after adsorption of propane 2-^{13}C contains the only resonance, at about 17.7 ppm, corresponding to the initially labelled methylene group of propane. After the sample was heated to 523 K, a small NMR line at ca. 19.5 ppm appeared; the origin of which is discussed later in the paper. Further heating to 548 and 573 K led to the appearance of labelled ethane ($\delta = 6.5$ ppm), the amount of which increased with increasing temperature. The labelled methane was observed only at 598 K ($\delta = -7.3$ ppm) along with ^{13}C label scrambling in propane, as evidenced by the line at ca. 16.2 ppm corresponding to the labelled methyl group in propane. Finally, at 623 K the NMR lines of propane disappeared, and the only observable signals corresponded to ethane and methane.

With propane 1-^{13}C used as a starting reactant (Fig. 4b), resonance at ca. 20.3 ppm instead of the peak at ca. 19.5 ppm was observed at the onset of the reaction. Moreover, labelled methane and ethane appeared simultaneously at 548 K in equimolar amounts, and selectivity to the labelled methane at the end of the reaction was higher than that found when using propane 2-^{13}C as the starting reactant.

The formation of equal amounts of initially labelled methane and ethane from propane 1-^{13}C and labelled ethane from

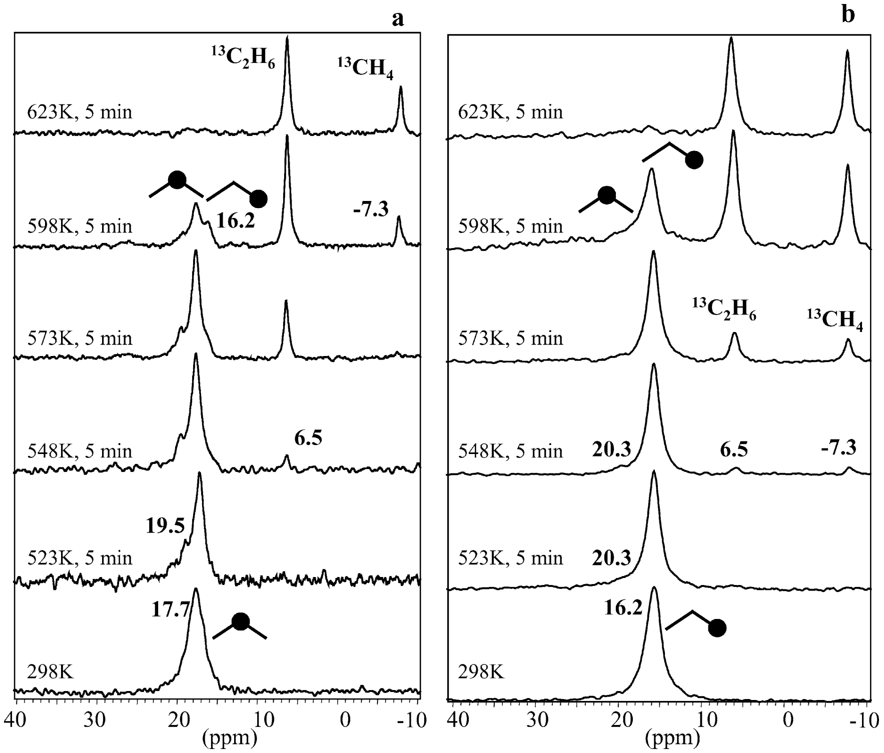

Fig. 4. $^{13}C\{^1H\}$ MAS NMR spectra observed in the course of propane 2-^{13}C (a) and propane 1-^{13}C(b) reactions over Zn/H-MFI catalyst.

propane-2-^{13}C points to propane hydrogenolysis at the initial steps of the reaction:

$$^{13}CH_3CH_2CH_3 + H_2 = {}^{13}CH_4 + CH_3CH_3,$$
$$^{13}CH_3CH_2CH_3 + H_2 = {}^{13}CH_3CH_3 + CH_4,$$
$$CH_3{}^{13}CH_2CH_3 + H_2 = CH_3{}^{13}CH_3 + CH_4.$$

This reaction pathway is significantly different that the pathways observed previously over H-MFI [16,23] and Ga/H-MFI [11a,11c,11e,12] catalysts. For comparison, Fig. 5 shows the ^{13}C MAS NMR spectra obtained during reaction of propane-2-^{13}C over the H-MFI and Ga/H-MFI samples, prepared from the same starting zeolite. The following differences emerge:

1. The reaction starts at much higher temperature (at 598 K on H-MFI and at 548 K on Ga/H-MFI).
2. The line at ca. 19.5 ppm is not observed at the onset of the reaction on either H-MFI or Ga/H-MFI.
3. The ^{13}C scrambling, evidenced by the appearance of the line corresponding to propane methyl group (16–17 ppm), is the only primary pathway of propane conversion.
4. Ethane is formed simultaneously with butanes, as evidenced by the lines at ca. 6.5, 24.0, and 26.0 ppm.

Therefore, it is evident that the mechanisms proposed previously for propane activation over H-MFI [16,23] and Ga/H-MFI [11a,11c,11e,12] catalysts cannot be transferred to Zn-containing catalysts. As mentioned earlier, the reaction pathway on the latter should involve propane hydrogenolysis. Such a reaction pathway can occur on Zn-containing species; however, the source of the dihydrogen required for this reaction is not clear. Understanding the nature of the intermediate species formed at the onset of the reaction may provide the key to answering this question.

To reveal the nature of the resonances at ca. 19.5 and 20.3 ppm, ^{1}H–^{13}C CP/MAS NMR spectra were recorded at the onset of propane 1-^{13}C and propane 2-^{13}C conversion over Zn/H-MFI (Fig. 6). The relative intensities of the lines at 19.5 and 20.3 ppm were significantly higher for the CP/MAS spectra compared with the $^{13}C\{^1H\}$ spectra, suggesting that these signals correspond to very rigid species attached to the zeolite surface. In addition, another line at ca. 12.2 ppm became visible during propane 1-^{13}C conversion.

In previous work [13], we suggested that such signals may correspond to propylene oligomers formed on propane dehydrogenation followed by propylene oligomerization over zeolite acid sites. To verify this suggestion, propylene 2-^{13}C and propylene 1-^{13}C were adsorbed over Zn/H-MFI and heated to 523 K (Fig. 7). The initial spectra obtained at ambient temperature indeed contained the lines at ca. 12 and 19–20 ppm, but the chemical shifts of these lines were not exactly the same as in the case of propane spectra (Fig. 6). Furthermore, the main resonance line, corresponding to propene oligomers, was observed at ca. 32.7 ppm, similar to the results of other research groups for propylene oligomers formed over acidic zeolites [24]. However, no such signal was detected in experiments with propane (Fig. 6). Finally, heating of the samples to 523 K caused cracking of the oligomers into propane and butanes, as evidenced by the lines at ca. 17.7 and 26.0 ppm, respectively (Fig. 7). But these lines were not detected at the onset of propane activation (Fig. 6); consequently, the hypothesis of propylene oligomer formation does not explain all of our results.

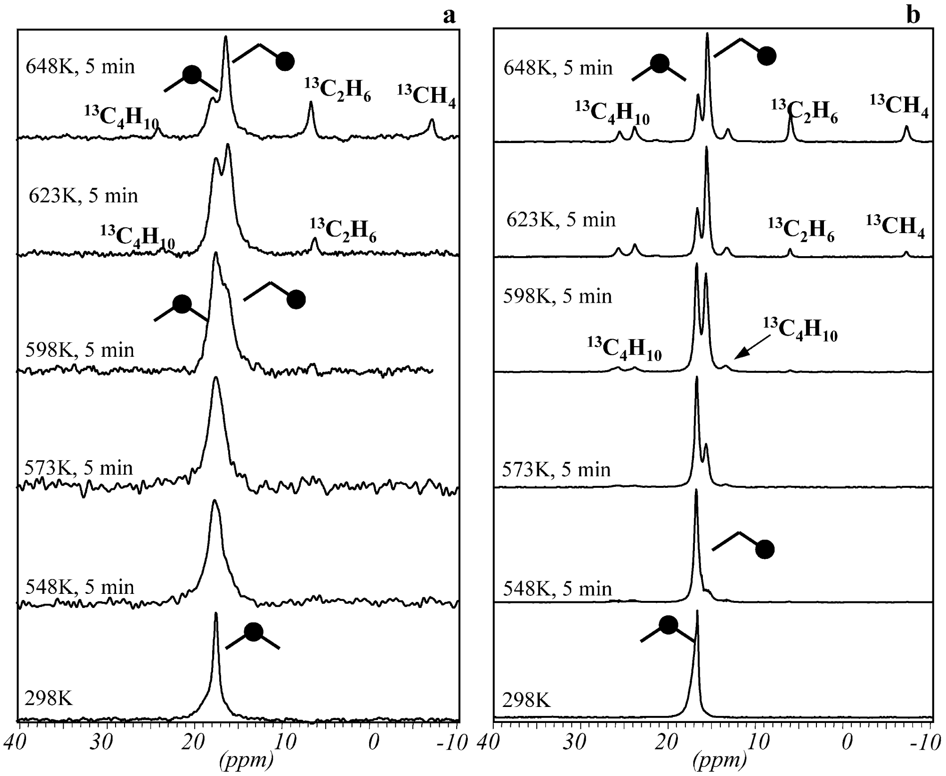

Fig. 5. $^{13}C\{^1H\}$ MAS NMR spectra observed in the course of propane 2-^{13}C reaction over H-MFI (a) and Ga/H-MFI (b) catalyst.

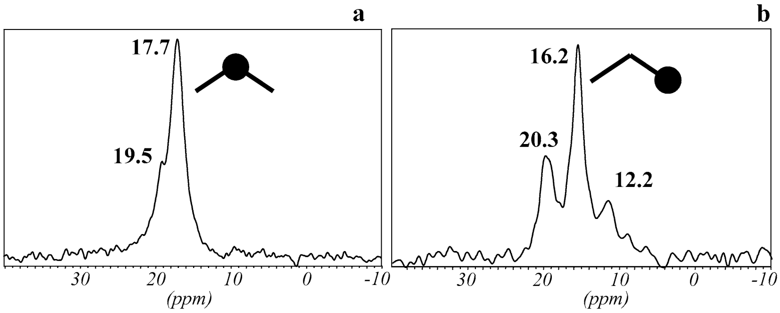

Fig. 6. ^1H–^{13}C CP/MAS NMR spectra observed after reaction of propane 2-^{13}C (a) and propane 1-^{13}C (b) over Zn/HMFI at 523K for 5 min.

To determine which active sites are responsible for the formation of the species corresponding to the lines at ca. 12.2 and 19–20 ppm, we carried out experiments over the catalysts containing only acidic (H-MFI) or only Zn sites (Zn-silicalite) (Fig. 8). Propane 1-^{13}C adsorbed over H-MFI did not show any new signals after heating at 523 K for 5 min (Fig. 8a). In contrast, the lines at ca. 20.3 and 12.2 ppm were observed over Zn/silicalite (Fig. 8b), similar to the findings of experiments over Zn/H-MFI (Fig. 7b). These results show unambiguously that Zn sites are responsible for the observed lines and suggest that the latter may correspond to the alkyl species attached to Zn sites.

Analysis of the chemical shifts of propyl groups attached to metal in different organometallic compounds [25–27] (Table 1) shows that the carbon atoms closest to metal are characterized by chemical shifts in the range of ca. 9–12, while the second and third atoms – by the chemical shifts in the range of 20–25 ppm. These findings suggest that the lines observed in our experiments can be indeed attributed to zinc propyl species. Our observation of the lines at ca. 12.2 and 20.3 ppm in the case of propane 1-^{13}C initially labelled in the methyl group and only one line at ca. 19.5 ppm in the case of propane 2-^{13}C indicates that the detected species more likely correspond to *n*-propyl zinc than to *iso*-propyl zinc species. Our NMR results thus point to propane activation through dissociative adsorption over zinc oxide species.

The dissociative adsorption of hydrogen and light alkanes has been addressed in the literature for both bulk zinc oxide [28] and Zn-modified MFI catalysts [21,29–31]. In early IR spectroscopic studies, Dent and Kokes [28] observed the formation of Zn–OH (3489 cm^{-1}) and Zn–H (1709 cm^{-1}) species on dihydrogen adsorption over bulk zinc oxide. These species were not very stable and were easily removed by recombinative desorption after evacuation procedure. Using DRIFT techniques, Kazansky et al. showed that dissociative adsorption of dihydrogen over HMFI modified by zinc vapor led to the

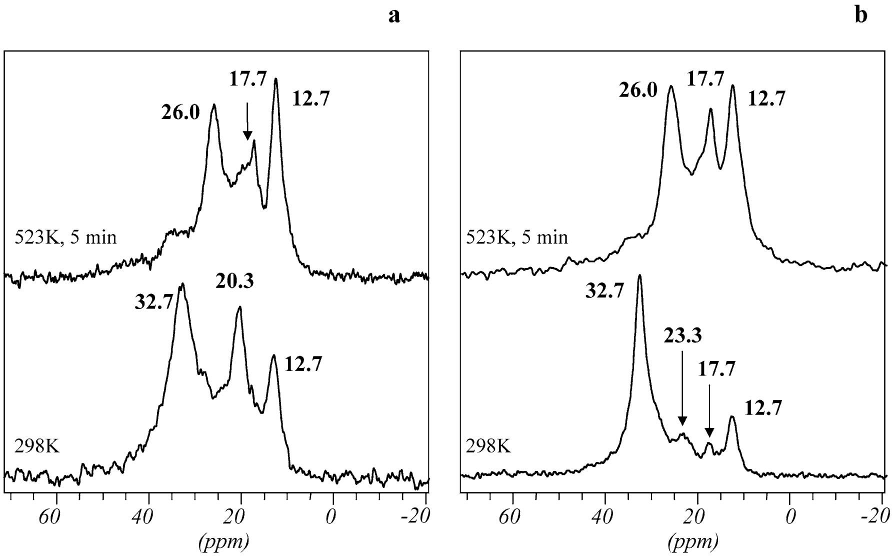

Fig. 7. ^{1}H–^{13}C CP/MAS NMR spectra observed after adsorption and reaction of propylene 1-^{13}C (a) and propylene 2-^{13}C (b) over Zn/HMFI.

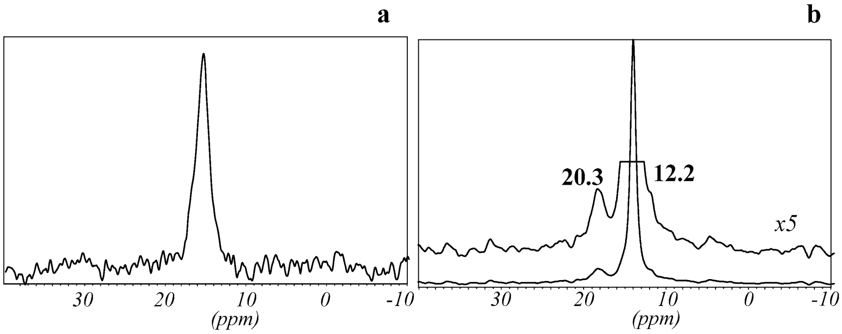

Fig. 8. ^{1}H–^{13}C CP/MAS NMR spectra observed after reaction of propane 1-^{13}C over HMFI (a) and (b) Zn/silicalite at 523 K for 5 min.

Table 1
^{13}C chemical shifts of propyl and isopropyl groups in organometallic compounds

Formula	Chemical shift of ^{13}C in $C_3H_7^+$ group (ppm)			Refs.
	C-1	C-2	C-3	
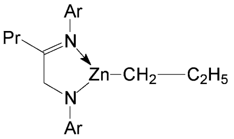	11.6–11.9	n/a	n/a	[25]
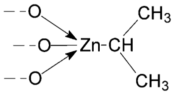	10.7	24.9	–	[26]
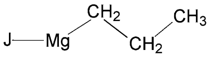	11.3	22.1	22.1	[27]
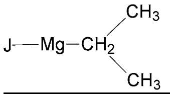	8.9	22.9	–	

formation of more stable hydroxyl SiOHAl (3610 cm^{-1}) and hydride (1934 cm^{-1}) species on zinc cations [30]. The same group also observed dissociative adsorption of methane and ethane [31] at moderately elevated temperatures over acid–base pairs with distantly separated Zn^{2+} cations and basic oxygen atoms of the zeolite framework in Zn/MFI catalysts with a high content of Zn^{2+} cations. In these studies, the simultaneous formation of acidic bridging hydroxyls SiOHAl (3610 cm^{-1}) and zinc ethyl (2874, 2910, 2958 cm^{-1}) or zinc methyl (2890, 2927, 2980 cm^{-1}) fragments was confirmed by DRIFT spectroscopy. The possibility of the dissociative adsorption of hydrogen, methane, and ethane over acid–base $Zn^{\delta+}$–$O^{\delta-}$ pairs has also been confirmed by theoretical studies [29].

It should be noted that dissociative adsorption has also been mentioned in the case of propane activation over Zn/MFI catalysts [21]; however, no direct experimental evidence of the presence of zinc propyl species has been provided. To the best of our knowledge, such information is not available for bulk zinc oxide as well. In contrast, there are data on zinc ethyl species formation over bulk zinc oxide. Thus, Dent and Kokes obtained direct evidence of the action of zinc ethyl species as intermediates of ethylene hydrogenation by gaseous hydrogen [32]. The formation of such species was detected and proven by IR spectroscopy.

To identify the positions of IR bands corresponding to zinc propyl species over zeolite catalysts modified by zinc oxide, we performed experiments similar to those carried out by Dent and Kokes [32] over Zn/silicalite catalyst. The experimental procedure included three steps: (1) conducting adsorption of propylene over Zn/silicalite at an equilibrium pressure of 2 Torr, followed by evacuation at ambient temperature; (2) subjecting the sample with strongly adsorbed propylene species to 100 Torr of hydrogen and heating it to selected temperature for a selected time; and (3) evacuating the resulting sample to observe strongly adsorbed species. In a series of experiments, the temperature of hydrogen interaction with adsorbed propylene was varied from 298 to 383 K; the results on propylene hydrogenation over Zn-silicalite are presented in Fig. 9.

The IR spectrum observed after adsorption of propylene and subsequent evacuation (Fig. 9, spectrum 1) shows four well-resolved bands in the 1350–1500 cm^{-1} region, at 1376 and 1451 cm^{-1} and at 1411 and 1428 cm^{-1}. These vibrations correspond to the CH_3 bending modes and in-plane deformation of the vinylic group, respectively. The preservation of the bands after evacuation points to strong propylene adsorption over Zn/silicalite catalyst. Subsequent adsorption of hydrogen at ambient temperature does not lead to any significant changes (spectrum not shown). Complete hydrogenation of adsorbed propylene into propane occurred only at 383 K, as evidenced by the appearance of the bands at 1370 and 1457 cm^{-1} and at 1385 and 1465 cm^{-1} (Fig. 9, spectrum 3), corresponding to the bending modes of CH_3 and CH_2 groups, respectively. Note that, in contrast to propylene, propane is weakly adsorbed and can be easily removed after evacuation (spectrum not shown). In the intermediate stage of hydrogenation, species characterized by five new bands at 1384, 1392, 1434, 1463, and 1469 cm^{-1} were detected (Fig. 9, spectrum 2). These bands belong to neither propylene nor propane; they show intermediate behaviour in propylene hydrogenation and correspond to species strongly attached to the surface, as confirmed by the preservation of their intensity on evacuation. In analogy with previous work [32], thee bands were attributed to zinc propyl species.

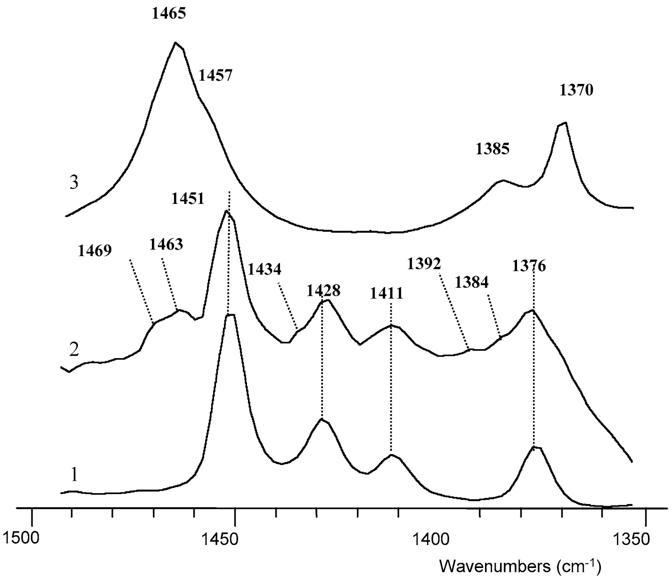

Fig. 9. FTIR spectra observed after adsorption of 2 Torr of propylene and evacuation at ambient temperature over Zn/silicalite (1), after consequent subjecting to 100 Torr of hydrogen and heating either at 373 K for 5 min with following evacuation (2) or at 383 K for 10 min without evacuation (3).

To verify whether these species are observed during propane activation over Zn-containing zeolites, we studied the initial stages of propane conversion over Zn/H-MFI and Zn/silicalite catalysts by IR spectroscopic techniques. Fig. 10 shows the IR spectra obtained in the range of 1320–1650 cm^{-1} after adsorption of propane at ambient temperature and after reaction at 523 K for 30 min and subsequent evacuation at ambient temperature over Zn/H-MFI (Fig. 10a) and Zn/silicalite (Fig. 10b), respectively. In the initial spectra, four bands at 1370, 1385, 1455, and 1465 cm^{-1}, corresponding to propane, were observed over both samples (Fig. 10a, spectra 1). Heating to 523 K produced no visible changes in the case of Zn/silicalite (Fig. 10b, spectrum 2). In the case of Zn/H-MFI, a weak band at 1587 cm^{-1} was detected (Fig. 10a, spectrum 2); this band could correspond to the stretching vibration of a C=C bond linked to Zn [33]. The evacuation of the samples at ambient temperature allowed observation of another strongly adsorbed species (Fig. 10, spectra 3,4). As mentioned earlier, the bands at 1376, 1411, 1428, 1451, and 1587 cm^{-1} corresponded to strongly adsorbed propylene over Zn-containing species, whereas weak bands at 1384,1392, 1434, 1463 and 1470 cm^{-1} can be attributed to the formation of zinc propyl species. The IR spectroscopic experiments thus confirm the formation of zinc propyl species at the onset of propane conversion. Moreover, propylene formation, which was not observed in the NMR experiments, was detected under the conditions of the IR experiments.

To help understand the mechanism of zinc propyl species formation further, considering the fate of the H-atom, which should be cleaved during dissociative adsorption of propane, could be helpful. The simplest hypothesis for this is that dissociation occurs hetrolytically, and the positively charged hydrogen atom moves to the oxygen atom, which is located close to Zn, forming an OH group. To prove this, the formation of new OH groups at the onset of propane conversion should be examined.

Because the amount of newly formed OH groups was rather low and the OH region of the spectrum was rather noisy, no definite conclusions about the appearance of new OH groups could be drawn from the IR spectroscopic experiments on propane conversion. Therefore, the same type of experiments were performed on deuterated samples with propane-D_8. The OD regions of the spectra recorded for initial Zn/H-MFI and Zn/silicalite catalysts, deuterated catalyst samples, and deuterated samples after reaction with deuterated propane are shown in Fig. 11.

No bands on the initial nondeuterated samples were detected in the OD region (Fig. 11, spectra 1). After H/D exchange with D_2O, bands at 2664, 2705–2710, and 2758 cm^{-1} appeared, corresponding to Si–OD–Al, Zn–OD, and Si–OD vibrations (Fig. 11, spectra 2). No bridging acidic sites were observed on Zn/silicalite. The reaction of C_3D_8 with deuterated zeolite samples at 523 K led to enhanced intensity of the band corresponding to Zn–OD (Fig. 11, spectra 3), as evidenced by the differences between the spectra of the initial deuterated sample and the sample after the reaction with propane (Fig. 11, spectra 4). This result indicates that propane dissociative adsorption occurs on zinc oxide species.

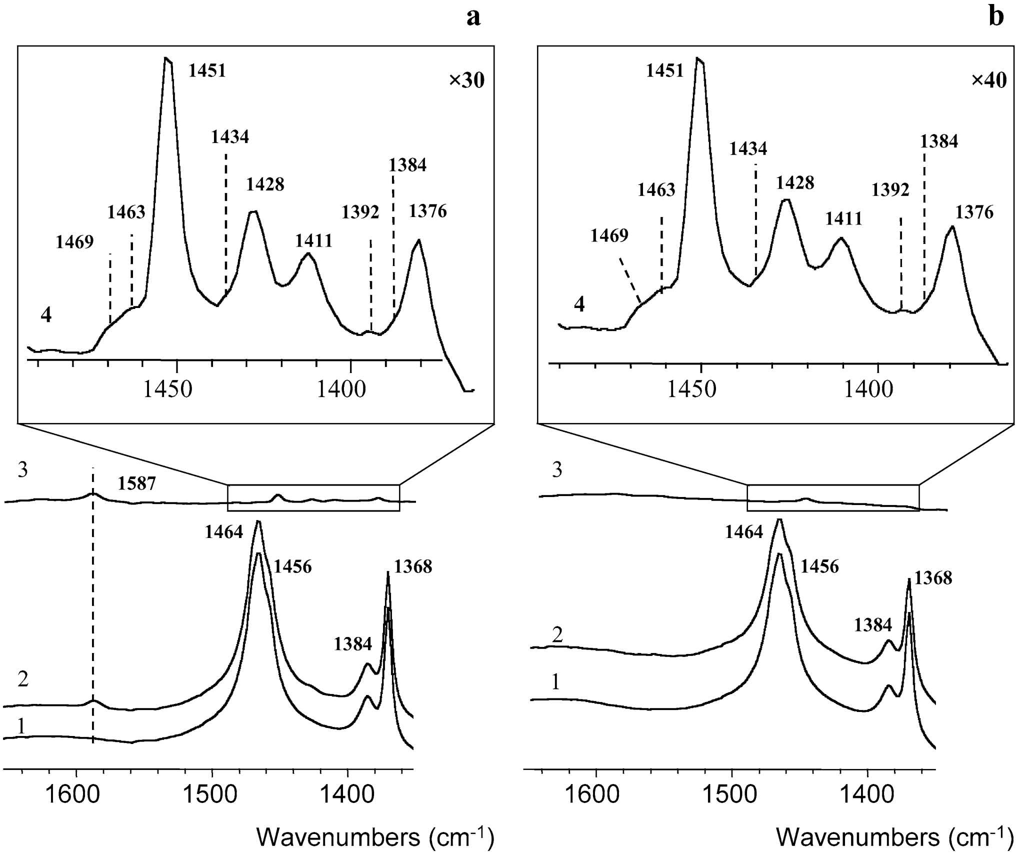

Fig. 10. FTIR spectra observed for reaction of propane over Zn/H-MFI (a) and Zn/silicalite (b) after propane adsorption (20 Torr) (1), after consequent heating at 523K for 30 min (2), and evacuation at ambient temperature (3). Spectrum 4 is enlarged part of spectrum 3.

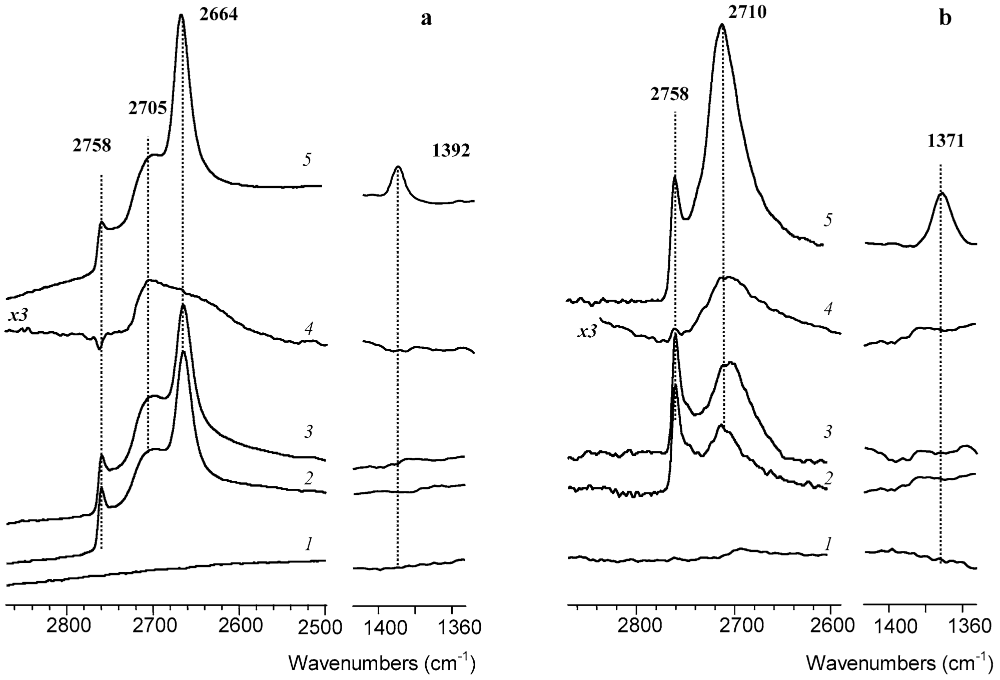

Fig. 11. FTIR spectra observed over Zn/H-MFI (a) and Zn/silicalite (b) in non-deuterated forms (1), in deuterated forms (2), after subjecting deuterated zeolites to 2 Torr of C_3D_8, heating at 523K for 30 min and evacuation (3) after subjecting of deuterated zeolites to 100 Torr of D_2 and evacuation at ambient temperature (5). Difference spectrum 4 is obtained by subtraction of spectrum 2 from spectrum 3.

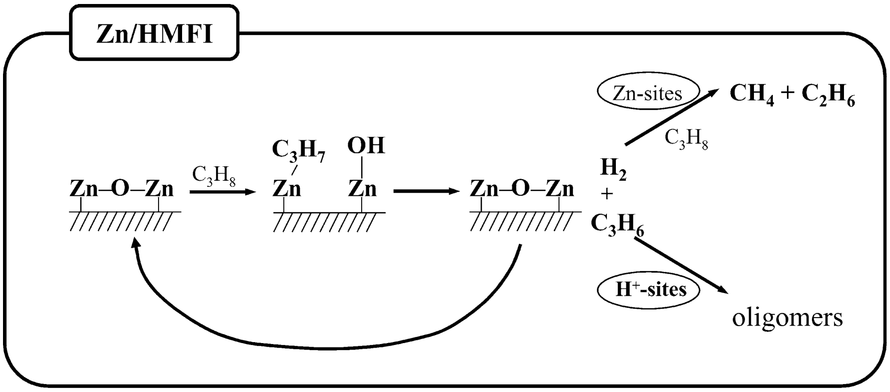

Fig. 12. Initial products and intermediates observed at the initial steps of propane reaction over Zn/HMFI catalyst.

Our results are somewhat different from the observations of Kazansky et al. [31] obtained during the investigation of dissociative adsorption of methane and ethane over Zn/MFI catalysts. Instead of the appearance of additional ZnOH groups, those authors observed an increased intensity of acidic bridging hydroxyls. Moreover, they found that dissociative adsorption occurred at lower temperatures, 473 K for methane and 423 K for ethane. These discrepancies could be due to the varying nature of the Zn species in the catalysts used for these studies. Whereas Kazansky et al. [31] used high-temperature reaction with zinc vapour to achieve greater incorporation of zinc in cationic positions, our samples were prepared by wet impregnation, leading to both zinc oxide species and zinc cations. Moreover, the content of Zn was four times higher in our studies. Consequently, in our samples the main part of zinc was in the form of oxide, in contrast to the samples of Kazansky et al. [31], in which special precautions were undertaken to ensure zinc incorporation in cationic positions of the zeolite. These factors explain why the reaction occurs on zinc oxide species in our samples, but on acid–base pairs with distantly separated Zn^{2+} cations and basic oxygen atoms of the zeolite framework in Kazansky et al.'s samples. The weaker strength of zinc oxide species further accounts for the higher temperature for propane dissociation required in our experiments.

To obtain more information on the sites involved in propane dissociation, we carried out additional experiments on the interaction of D_2 with the same zeolites (Fig. 11, spectrum 5). Similar to the experiments with deuterated propane, the intensity of the band corresponding to Zn–OD groups increased. In addition, new bands at 1371 and 1391 cm^{-1} appeared simultaneously with the Zn–OD-groups over Zn/silicalite and Zn/H-MFI catalysts, respectively. These bands could be due to Zn–D-species. Indeed, the wavenumbers of these bands are in good agreement with the value of 1934 cm^{-1} obtained for Zn–H species by Kazansky [30]. The values differ by only an isotope shift constant (around 0.7). These experiments suggest that D_2 dissociative adsorption also occurs on zinc oxide species on our catalysts. The observation of Zn–D bands only with D_2 confirms that in the case of propane, zinc sites are occupied by propyl species.

It should be mentioned that binuclear ions with bridging oxygen $(OZ)^-(Zn–O–Zn)^{2+}(OZ)^-$, which are possibly present in our Zn/H-MFI sample, may also be responsible for the formation of zinc propyl species and generation of ZnOH groups in this catalyst. Further work is needed to identify the role of different cations in propane dissociation, and such investigations currently underway in our laboratories.

In summary, the results of ^{13}C MAS NMR and IR spectroscopic in situ studies point to the formation of zinc propyl and ZnOH groups at the onset of propane reaction over Zn/H-MFI catalysts with high zinc content. These findings demonstrate that the initial step of propane conversion over Zn-containing zeolites is dissociative adsorption over Zn oxide species.

The overall reaction mechanism presented in Fig. 12 rationalizes all of the foregoing observations. The first step in propane activation over Zn/H-MFI is dissociative adsorption over zinc oxide sites, leading to the formation of propyl zinc species and Zn–OH groups. The subsequent dehydrogenation of propyl groups and recombination of hydrogen over Zn sites leads to propylene and dihydrogen formation and regeneration of an active catalytic site. Propylene undergoes further oligomerization over the neighbouring acidic site, whereas dihydrogen may participate in propane hydrogenolysis under certain reaction conditions. Thus, under the batch conditions of the NMR experiment, implying elevated pressures, dihydrogen participates in propane hydrogenolysis to methane and ethane over Zn sites. Under the conditions of IR experiments or continuous-flow experiments [10], implying lower or ambient pressures, dihydrogen is a final reaction product. The recombinative hydrogen desorption shifts the reaction equilibrium toward propylene formation, which further undergoes oligomerization, cyclization, and aromatisation, accounting for the higher aromatization activity of Zn-containing zeolites with respect to pure acidic sites.

The mechanism proposed for propane activation over Zn/H-MFI catalysts is quite different from those proposed previously [11a,11c,11e,12] for Ga/H-MFI catalysts. On Ga/H-MFI, the acidic and Ga sites purportedly work in synergy at the very early stages of propane activation, leading to the cyclic PPCP intermediate, accounting for ^{13}C scrambling in propane as the main reaction pathway. In contrast, on Zn/H-MFI catalysts, only Zn sites are found to be responsible for the initial propane activation, leading to propane dissociative adsorption and dehydrogenation, while acidic sites participate in subsequent reaction steps, such as propene oligomerization, cyclization, and so on. Zn sites are also very active in propane hydrogenolysis, accounting for the ethane and methane formation at the very early stages of the reaction. These findings explain the higher activity of Zn/H-MFI catalysts in propane conversion and the lower selectivity toward aromatics, due to the enhanced ethane and methane formation [34].

4. Conclusion

In situ ^{13}C MAS NMR and IR spectroscopic techniques revealed zinc propyl species at the onset of propane conversion over Zn/H-MFI catalyst. Simultaneous formation of ZnOH groups was evidenced by IR spectroscopic techniques. The results were accounted for by propane dissociative adsorption over zinc oxide species.

The mechanism proposed for propane activation involves propane dissociation, followed by propene evolution and recombinative desorption of dihydrogen. Propene further oligomerizes over acidic sites, while dihydrogen either evolves as a final product or participates in propane hydrogenolysis into ethane and methane. At low partial pressure of the reactants, H_2 recombinative desorption and hydrogen evolution is favoured, whereas at high pressures, implied under NMR batch conditions, the hydrogenolysis route is preferred. This mechanistic pathway explains the higher activity of Zn/H-MFI catalysts with respect to H-MFI and the lower selectivity to aromatics in comparison to Ga/H-MFI.

Acknowledgments

The authors thank INTAS Programme for research grants. I.I. Ivanova is grateful to RFBR for financial support. Yu.G. Kolyagin thanks Haldor Topsoe A/S for a doctoral fellowship.

References

[1] (a) Y. Ono, K. Kanae, J. Chem. Soc., Faraday Trans. 87 (1991) 669;
(b) Y. Ono, Catal. Rev.-Sci. Eng. 34 (1992) 179.
[2] (a) N.S. Gnep, J.Y. Doyemet, M. Guisnet, J. Mol. Catal. 45 (1988) 281;
(b) N.S. Gnep, J.Y. Doyemet, A.M. Seco, F.R. Ribeiro, M. Guisnet, Appl. Catal. 43 (1988) 155;
(c) M. Guisnet, N.S. Gnep, F. Alario, Appl. Catal. A 89 (1992) 1;
(d) M. Guisnet, D. Lukyanov, Acid–Base Catalysis, Elsevier, Amsterdam, 1994, p. 367;
(e) G. Giannetto, A. Montes, N.S. Gnep, A. Florentino, P. Cartraud, M. Guisnet, J. Catal. 145 (1994) 86;
(f) M. Guisnet, N.S. Gnep, Catal. Today 31 (1996) 275.
[3] G.L. Price, V. Kanazirev, K.M. Dooley, V.I. Hart, J. Catal. 173 (1998) 17.
[4] T. Mole, J.R. Anderson, G. Creer, Appl. Catal. 17 (1985) 141.
[5] V.B. Kazansky, V.Y. Borovkov, A.I. Serikh, R.A. van Santen, B.G. Anderson, Catal. Lett. 66 (2000) 39.
[6] (a) P. Meriaudeau, C. Naccache, Catal. Today 31 (1996) 265;
(b) P. Meriaudeau, S.B.A. Hamid, C. Naccache, J. Catal. 139 (1993) 679.
[7] (a) G. Buckles, G.J. Hutchings, C.D. Williams, Catal. Lett. 11 (1991) 89;
(b) G. Buckles, G.J. Hutchings, C.D. Williams, Catal. Lett. 8 (1991) 115.
[8] T. Inui, F. Okazumi, J. Catal. 90 (1984) 366.
[9] (a) R. le van Mao, L. Dufresne, Appl. Catal. 52 (1989) 1;
(b) R. le van Mao, J. Yao, B. Sjiariel, Catal. Lett. 6 (1990) 23;
(c) R. le van Mao, J.H. Yao, Appl. Catal. 79 (1991) 77;
(d) R. le van Mao, J.H. Yao, L.A. Dufresne, R. Carli, Catal. Today 31 (1996) 247;
(e) R. le van Mao, L. Dufresne, J.H. Yao, Appl. Catal. 65 (1990) 143;
(f) L.A. Dufresne, R. le van Mao, Catal. Lett. 25 (1994) 371;
(g) J. Yao, R. le van Mao, L. Dufresne, Appl. Catal. 65 (1990) 175;
(h) L. Dufresne, J. Yao, R. Levanmao, Abstr. Pap. Am. Chem. Soc. 199 (1990) 140.
[10] (a) E. Iglesia, J.E. Baumgartner, G.L. Price, J. Catal. 134 (1992) 549;
(b) E. Iglesia, J.E. Baumgartner, Catal. Lett. 21 (1993) 55;
(c) J.A. Biscardi, E. Iglesia, Catal. Today 31 (1996) 207;
(d) S.Y. Yu, J.A. Biscardi, E. Iglesia, J. Phys. Chem. B 106 (2002) 9642;
(e) J.A. Biscardi, E. Iglesia, J. Catal. 182 (1999) 117;
(f) J.A. Biscardi, E. Iglesia, Phys. Chem. Chem. Phys. 1 (1999) 5753.
[11] (a) I. I Ivanova, E.G. Derouane, Advanced Zeolite Science and Applications, Elsevier, Amsterdam, 1994, p. 357;
(b) J.F. Haw, Top. Catal. 8 (1999) 81;
(c) I.I. Ivanova, Colloids Surf. A 158 (1999) 189;
(d) A.G. Stepanov, Uspekhi Khimii 68 (1999) 619;
(e) E.G. Derouane, H.Y. He, S. Hamid, D. Lambert, I.I. Ivanova, J. Mol. Catal. A 158 (2000) 5;
(f) M. Hunger, J. Weitkamp, Angew. Chem. Int. Ed. 40 (2001) 2954;
(g) W.O. Parker, Comments Inorg. Chem. 22 (2000) 31;
(h) X.W. Han, Z.M. Yan, W.P. Zhang, X.H. Bao, Curr. Org. Chem. 5 (2001) 1017;
(i) J.F. Haw, Phys. Chem. Chem. Phys. 4 (2002) 5431.
[12] (a) E.G. Derouane, S.B.A. Hamid, I.I. Ivanova, N. Blom, P.E. Hojlund-nielsen, J. Mol. Catal. 86 (1994) 371;
(b) I.I. Ivanova, N. Blom, S.B.A. Hamid, E.G. Derouane, Recl. Trav. Chim. Pays-Bas. 113 (1994) 454;
(c) I.I. Ivanova, N. Blom, E.G. Derouane, J. Mol. Catal. 109 (1996) 157.
[13] Y.G. Kolyagin, J. Quartararo, E.G. Derouane, F. Fajula, I.I. Ivanova, in: E.G. Derouane, V.N. Parmon, F. Lemos, F. Ramoa Ribeiro (Eds.), NATO SS, 191, 2005, p. 333.
[14] C.R. Morcombe, K.W. Zilm, J. Magn. Reson. 162 (2003) 479.
[15] W.L. Earl, D.L. Vanderhart, J. Magn. Reson. 48 (1982) 35.
[16] I.I. Ivanova, E.B. Pomakhina, A.I. Rebrov, E.G. Derouane, Top. Catal. 6 (1998) 49.
[17] El.-M. El-Malki, R.A. van Santen, W.M.H. Sachtler, J. Phys. Chem. B 103 (1999) 4611.
[18] J. Chen, Z. Feng, P. Ying, C. Li, J. Phys. Chem. B 108 (2004) 12669.
[19] A.L. Lapidus, A.A. Dergachev, V.A. Kostina, I.V. Mishin, Izv. Acad. Nauk 5 (2005) 1035.
[20] G.L. Griffin, G.T. Yates, J. Chem. Phys. 77 (1982) 3751.
[21] V.B. Kazansky, V.Yu. Borovkov, A.I. Serikha, R.A. van Santen, B.G. Anderson, Catal. Lett. 66 (2000) 39.
[22] J.A. Biscardi, G.D. Meitzner, E. Iglesia, J. Catal. 179 (1998) 192.
[23] (a) I.I. Ivanova, N. Blom, E.G. Derouane, Stud. Surf. Sci. Catal. 94 (1995) 419;
(b) I.I. Ivanova, A.I. Rebrov, E.B. Pomakhina, E.G. Derouane, J. Mol. Catal. A 141 (1999) 107.
[24] (a) J.F. Haw, B.R. Richardson, I.S. Oshiro, N.D. Lazo, J.A. Speed, J. Am. Chem. Soc. 111 (1989) 2052;
(b) J.L. White, N.D. Lazo, B.R. Richardson, J.F. Haw, J. Catal. 125 (1990) 260.
[25] E. Wissing, K. van Gorp, J. Boersma, G. van Koten, Inorg. Chim. Acta 220 (1994) 55.
[26] A. Looney, M. Cornebise, D. Miller, G. Parkin, Inorg. Chem. 31 (1992) 989.
[27] E. Breimaier, W. Voelter, Carbon-13 NMR Spectroscopy: High-Resolution Methods and Applications in Organic and Biochemistry, VCH, New York, 1990, p. 515.
[28] (a) L. Dent, R.J. Kokes, J. Am. Chem. Soc. 92 (1970) 6709;
(b) R.J. Kokes, C.C. Chang, L.T. Dixon, A.L. Dent, J. Am. Chem. Soc. 94 (1972) 4429.
[29] (a) A.A. Shubin, G.M. Zhidomirov, V.B. Kazansky, R.A. van Santen, Catal. Lett. 90 (2003) 137;
(b) V.B. Kazanskii, E.A. Pid'ko, Kinet. Catal. 43 (2002) 567;
(c) L. Barbosa, R.A. van Santen, J. Phys. Chem. B 107 (2003) 4532;

(d) L. Barbosa, G.M. Zhidomirov, R.A. van Santen, Catal. Lett. 77 (2001) 55;
(e) L. Barbosa, G.M. Zhidomirov, R.A. van Santen, Phys. Chem. Chem. Phys. 2 (2000) 3909;
(f) M.V. Frash, R.A. van Santen, Phys. Chem. Chem. Phys. 2 (2000) 1085;
(g) A.L. Yakovlev, A.A. Shubin, G.M. Zhidomirov, R.A. van Santen, Catal. Lett. 70 (2000) 175;
(h) N.U. Zhanpeisov, G.M. Zhidomirov, M. Baerns, J. Mol. Catal. A 99 (1995) 35.

[30] (a) V.B. Kazansky, A.I. Serykh, Phys. Chem. Chem. Phys. 6 (2004) 3760;
(b) V.B. Kazansky, A. Serykh, Microporous Mesoporous Mater. 70 (2004) 151.

[31] (a) V.B. Kazansky, A.I. Serykh, E.A. Pidko, J. Catal. 225 (2004) 369;
(b) V.B. Kazansky, E.A. Pidko, J. Phys. Chem. B 109 (2005) 2103.

[32] A.L. Dent, R.J. Kokes, J. Phys. Chem. 74 (1970) 3653.

[33] H.D. Kaesz, F.G.A. Stone, Spectrochim. Acta 15 (1959) 360.

[34] A. Corma, A. Martinez, in: M. Guisnet, J.P. Gilson (Eds.), Catalytic Science Series, 3, 2002, p. 29.